αIIb-W995/β3-transfected CHO cells exhibited membrane ruffling and abnormal cytoplasmic protrusions with the bulbous tips on fibrinogen-coated surfaces (Figure 1G), indicating that the salt bridge-disrupting mutations exert the same influence on the integrin activation and cytoskeletal events. Abnormal clustering of αIIbβ3, which was reported in *ITGB3* L718P mutation,[10] was not observed in these cells or in platelets spread on immobilized fibrinogen (supplemental Figure 1). It is worth noting that macrothrombocytopenia-associated *ITGB3* mutations in the ectodomain and the cytoplasmic membrane-proximal region have different properties in terms of outside-in signaling and bleeding tendency.[9,10]

Finally, to determine the functional consequences of R995W mutation on platelet production, we coexpressed αIIb and β3 in mouse fetal liver cells by retroviral transfer and differentiated them into megakaryocytes (Figure 1H). There was an early increase and decrease in the percentage of proplatelet formation-positive megakaryocytes in αIIb-W995/β3-transfected megakaryocytes. The number of proplatelet tips was decreased, and the size of the tips increased. These results are consistent with thrombocytopenia and the increased platelet size in patients, indicating that the stimulation of mutant αIIbβ3 leads to abnormal proplatelet formation. However, not all *ITGA2B*- and *ITGB3*-activating mutations are associated with macrothrombocytopenia. Patients with homozygous *ITGB3* C549R or C560R mutation inducing constitutively active αIIbβ3 have a normal platelet count and size,[23,24] suggesting different molecular mechanisms for the induction of abnormal proplatelet formation.

αIIbβ3 has not been implicated in an abnormal platelet count or morphology.[5] Our data support and extend the recent reports that heterozygous, activating mutations in *ITGA2B* and *ITGB3*, in the juxtamembrane region, cause macrothrombocytopenia.[6-10] We thus propose that such mutations represent the etiology of a subset of congenital macrothrombocytopenias. It is also probable that homozygosity causes Glanzmann thrombasthenia, as demonstrated in the original report of macrothrombocytopenia-associated *ITGA2B* R995Q mutation.[6,7] The creation of a knock-in mouse model and/or use of an in vivo megakaryocyte infusion model[25] should clarify the mechanism underlying the production and processing of giant platelets.

Acknowledgments

The authors thank Dr R. C. Mulligan (Children's Hospital Boston, Harvard Medical School, Boston, MA) for 293gp and 293gpg cells, Dr M. Handa (Department of Transfusion Medicine & Cell Therapy, Keio University School of Medicine, Tokyo, Japan) for PT25-2 antibodies, Dr A. Saito (Department of Clinical Research Promotion, Clinical Research Center, National Hospital Organization Nagoya Medical Center) for statistical analysis, and Yoshimi Ito-Yamamura for her skillful technical assistance.

This work was supported by the Japan Society for the Promotion of Science (Grant-in-Aid for Scientific Research), the Ministry of Health, Labor and Welfare, Academic Frontier Project in Japan, Mitsubishi Pharma Research Foundation, the 24th General Assembly of the Japanese Association of Medical Sciences Promotion Fund, the Mother and Child Health Foundation, and the National Hospital Organization Research Fund.

Authorship

Contribution: S.K. designed and performed research, analyzed data, and wrote the paper; H.K. and Y. Tomiyama performed platelet experiments and interpreted the results; M. Onodera constructed retrovirus vectors; M. Otsu, N.T., K.E., and M. Onodera designed the retroviral transfection experiments; Y.M., Y. Takamatsu, J.S., and K.M. contributed patient samples; and H.S. supervised the research.

Conflict-of-interest disclosure: The authors declare no competing financial interests.

Correspondence: Shinji Kunishima, Department of Advanced Diagnosis, Clinical Research Center, National Hospital Organization Nagoya Medical Center, 4-1-1 Sannomaru, Naka-ku, Nagoya 4600001, Japan; e-mail: kunishis@nnh.hosp.go.jp.

References

1. Balduini CL, Cattaneo M, Fabris F, et al. Inherited thrombocytopenias: a proposed diagnostic algorithm from the Italian Gruppo di Studio delle Piastrine. *Haematologica.* 2003;88(5):582-592.
2. Balduini CL, Savoia A. Inherited thrombocytopenias: molecular mechanisms. *Semin Thromb Hemost.* 2004;30(5):513-523.
3. Kunishima S, Saito H. Congenital macrothrombocytopenias. *Blood Rev.* 2006;20(2):111-121.
4. Nurden P, Nurden AT. Congenital disorders associated with platelet dysfunctions. *Thromb Haemost.* 2008;99(2):253-263.
5. Nurden AT. Glanzmann thrombasthenia. *Orphanet J Rare Dis.* 2006;1:10.
6. Hardisty R, Pidard D, Cox A, et al. A defect of platelet aggregation associated with an abnormal distribution of glycoprotein IIb-IIIa complexes within the platelet: the cause of a lifelong bleeding disorder. *Blood.* 1992;80(3):696-708.
7. Peyruchaud O, Nurden AT, Milet S, et al. R to Q amino acid substitution in the GFFKR sequence of the cytoplasmic domain of the integrin IIb subunit in a patient with a Glanzmann's thrombasthenia-like syndrome. *Blood.* 1998;92(11):4178-4187.
8. Ghevaert C, Salsmann A, Watkins NA, et al. A nonsynonymous SNP in the ITGB3 gene disrupts the conserved membrane-proximal cytoplasmic salt bridge in the alphaIIbbeta3 integrin and co-segregates dominantly with abnormal proplatelet formation and macrothrombocytopenia. *Blood.* 2008;111(7):3407-3414.
9. Gresele P, Falcinelli E, Giannini S, et al. Dominant inheritance of a novel integrin beta3 mutation associated with a hereditary macrothrombocytopenia and platelet dysfunction in two Italian families. *Haematologica.* 2009;94(5):663-669.
10. Jayo A, Conde I, Lastres P, et al. L718P mutation in the membrane-proximal cytoplasmic tail of beta3 promotes abnormal alphaIIbbeta3 clustering and lipid microdomain coalescence, and associates with a thrombasthenia-like phenotype. *Haematologica.* 2010;95(7):1158-1166.
11. Kunishima S, Hamaguchi M, Saito H. Differential expression of wild-type and mutant NMMHC-IIA polypeptides in blood cells suggests cell-specific regulation mechanisms in MYH9 disorders. *Blood.* 2008;111(6):3015-3023.
12. Kunishima S, Lopez JA, Kobayashi S, et al. Missense mutations of the glycoprotein (GP) Ibbeta gene impairing the GPIb alpha/beta disulfide linkage in a family with giant platelet disorder. *Blood.* 1997;89(7):2404-2412.
13. Kashiwagi H, Tomiyama Y, Tadokoro S, et al. A mutation in the extracellular cysteine-rich repeat region of the beta3 subunit activates integrins alphaIIbbeta3 and alphaVbeta3. *Blood.* 1999;93(8):2559-2568.
14. Kashiwagi H, Shiraga M, Kato H, et al. Expression and subcellular localization of WAVE isoforms in the megakaryocyte/platelet lineage. *J Thromb Haemost.* 2005;3(2):361-368.
15. Sanuki S, Hamanaka S, Kaneko S, et al. A new red fluorescent protein that allows efficient marking of murine hematopoietic stem cells. *J Gene Med.* 2008;10(9):965-971.
16. Suzuki A, Obi K, Urabe T, et al. Feasibility of ex vivo gene therapy for neurological disorders using the new retroviral vector GCDNsap packaged in the vesicular stomatitis virus G protein. *J Neurochem.* 2002;82(4):953-960.
17. Ory DS, Neugeboren BA, Mulligan RC. A stable human-derived packaging cell line for production of high titer retrovirus/vesicular stomatitis virus G pseudotypes. *Proc Natl Acad Sci U S A.* 1996;93(21):11400-11406.
18. Poncz M, Eisman R, Heidenreich R, et al. Structure of the platelet membrane glycoprotein IIb: homology to the alpha subunits of the vitronectin and fibronectin membrane receptors. *J Biol Chem.* 1987;262(18):8476-8482.

19. Kunishima S, Kobayashi R, Itoh TJ, Hamaguchi M, Saito H. Mutation of the beta1-tubulin gene associated with congenital macrothrombocytopenia affecting microtubule assembly. *Blood.* 2009;113(2):458-461.

20. Hughes PE, Diaz-Gonzalez F, Leong L, et al. Breaking the integrin hinge: a defined structural constraint regulates integrin signaling. *J Biol Chem.* 1996;271(12):6571-6574.

21. Lau TL, Kim C, Ginsberg MH, Ulmer TS. The structure of the integrin alphaIIbbeta3 transmembrane complex explains integrin transmembrane signalling. *EMBO J.* 2009;28(9):1351-1361.

22. Schaffner-Reckinger E, Salsmann A, Debili N, et al. Overexpression of the partially activated alphaIIbbeta3D723H integrin salt bridge mutant downregulates RhoA activity and induces microtubule-dependent proplatelet-like extensions in Chinese hamster ovary cells. *J Thromb Haemost.* 2009;7(7):1207-1217.

23. Mor-Cohen R, Rosenberg N, Peretz H, et al. Disulfide bond disruption by a beta3-Cys549Arg mutation in six Jordanian families with Glanzmann thrombasthenia causes diminished production of constitutively active alphaIIbbeta3. *Thromb Haemost.* 2007;98(6):1257-1265.

24. Ruiz C, Liu CY, Sun QH, et al. A point mutation in the cysteine-rich domain of glycoprotein (GP) IIIa results in the expression of a GPIIb-IIIa (alphaIIbbeta3) integrin receptor locked in a high-affinity state and a Glanzmann thrombasthenia-like phenotype. *Blood.* 2001;98(8):2432-2441.

25. Fuentes R, Wang Y, Hirsch J, et al. Infusion of mature megakaryocytes into mice yields functional platelets. *J Clin Invest.* 2010;120(11):3917-3922.

J Gastroenterol (2011) 46:779–789
DOI 10.1007/s00535-011-0380-3

ORIGINAL ARTICLE—LIVER, PANCREAS, AND BILIARY TRACT

Potent in vitro and in vivo antitumor activity of sorafenib against human intrahepatic cholangiocarcinoma cells

Hiroaki Sugiyama · Kenichiro Onuki · Kazunori Ishige · Nobue Baba · Tetsuya Ueda · Sachiko Matsuda · Kaoru Takeuchi · Masafumi Onodera · Yasuni Nakanuma · Masayuki Yamato · Masakazu Yamamoto · Ichinosuke Hyodo · Junichi Shoda

Received: 2 November 2010 / Accepted: 20 January 2011 / Published online: 18 February 2011

Abstract
Background Intrahepatic cholangiocarcinoma (ICC) is rising in clinical importance due to the increasing incidence worldwide, poor prognosis, and suboptimal response to therapies. New effective therapeutic approaches are needed for improvement of treatment outcome. A recent study showed that sorafenib, a multikinase inhibitor that acts predominantly through inhibition of Raf kinase and vascular endothelial growth factor (VEGF) and platelet-derived growth factor (PDGF) receptors, exhibited potent antitumor activity in a preclinical model of cholangiocarcinoma cells.
Method We tested the in vitro and in vivo antitumor activity of sorafenib against human ICC cell lines.
Results Treatment of ICC cells with sorafenib resulted in inhibition of proliferation and induction of apoptosis in the cell lines. In the cells treated with sorafenib, phosphorylation of mitogen-activated protein kinase kinase (MEK) and mitogen-activated protein kinase (MAPK) and also interleukin-6-induced phosphorylation of signal transducer and activator of transcription 3 (STAT3) were inhibited in a dose-dependent manner. Down-regulation of the anti-apoptotic protein myeloid cell leukemia-1 (Mcl-1) paralleled the reduced phosphorylation of STAT3. However, sorafenib induced no significant change in the cell cycle distribution and the expression levels of cyclin D1 and $p27^{Kip1}$ in the cells. For the in vivo antitumor activity, oral administration of sorafenib significantly inhibited the growth of subcutaneous tumors established in immunodeficient mice at doses of 10, 30, and 100 mg/kg. Moreover, administration of sorafenib (30 mg/kg) to animals with peritoneally disseminated ICC resulted in significantly

H. Sugiyama · K. Ishige · I. Hyodo · J. Shoda
Department of Gastroenterology, Institute of Clinical Medicine, University of Tsukuba Graduate School of Comprehensive Human Sciences, Tsukuba, Ibaraki, Japan

K. Onuki · M. Yamamoto
Department of Surgery, Institute of Gastroenterology, Tokyo Women's Medical University, Shinjuku-ku, Tokyo, Japan

N. Baba · T. Ueda
Pharmacodynamics Group, Drug Development Service Division, Medi-Chem Business Segment, Itabashi-ku, Tokyo, Japan

S. Matsuda
Department of Surgery, School of Medicine, Keio University, Shinjuku-ku, Tokyo, Japan

K. Takeuchi
Department of Infection Biology, Institute of Basic Medical Science, University of Tsukuba Graduate School of Comprehensive Human Sciences, Tsukuba, Ibaraki, Japan

M. Onodera
Department of Genetics, National Research Institute for Child Health and Development, Setagaya-ku, Tokyo, Japan

Y. Nakanuma
Department of Human Pathology, Graduate School of Medical Science, Kanazawa University, Kanazawa, Japan

M. Yamato
Institute of Advanced Biomedical Engineering and Science, Tokyo Women's Medical University, Shinjuku-ku, Tokyo, Japan

J. Shoda (✉)
Field of Basic Sports Medicine, Sports Medicine, University of Tsukuba Graduate School of Comprehensive Human Sciences, Tsukuba, Ibaraki, Japan
e-mail: shodaj@md.tsukuba.ac.jp

prolonged survival compared with that of untreated animals (76 vs. 43 days in treated and vehicle-treated mice, respectively).

Conclusion These results indicate that sorafenib is a potent agent that may provide a new therapeutic option for human ICC.

Keywords Cholangiocarcinoma · Molecular targeting therapy · Multi-tyrosine kinase inhibitor · Antitumor activity · Preclinical study

Abbreviations

Ab	Antibody
AKT/PKB	Protein kinase B
CC	Cholangiocarcinoma
IH	Intrahepatic
IL-6	Interleukin-6
JAK	Janus kinase
MAPK	Mitogen-activated protein kinase
Mcl-1	Myeloid cell leukemia-1
MEK	Mitogen-activated protein kinase kinase
STAT	Signal transducer and activator of transcription

Introduction

The incidence and mortality rates for intrahepatic cholangiocarcinoma (ICC) have been steadily increasing worldwide, with notable increases being reported in the USA, the UK, and Asia including Japan [1, 2]. Known risk factors are primary sclerosing cholangitis, liver fluke infestations, and hepatolithiasis [2]. Recent studies suggested that chronic hepatitis C infection and non-alcoholic steatohepatitis, especially when combined with cirrhosis, also contribute to cholangiocarcinogenesis in the intrahepatic bile ducts [3]. However, the reason for the increasing incidence of ICC remains unclear.

Despite advances in tumor biology, diagnostic imaging, adjuvant therapies, and surgical techniques, the survival of ICC patients remains dismal [4, 5]. Without early resection, these tumors invade adjacent vascular structures and liver parenchyma, extend along the bile duct epithelia, metastasize to the lymph nodes, and disseminate into the peritoneal space. The mainstay of treatment for ICC is complete resection with negative surgical margins. Under these circumstances, however, the role of adjuvant therapy is not well defined, and the benefits of palliative chemotherapy or chemoradiation for patients with unresectable disease have not been established. An effective new approach against this aggressive disease is urgently needed.

Recently, a number of multi-targeted tyrosine kinase inhibitors have been developed and used in clinical trials for cancer therapy [6]. Sorafenib (BAY43-9006, Nexavar) is an oral multikinase inhibitor that was developed as a c-Raf kinase inhibitor. It also targets several other Raf kinases as well as receptor tyrosine kinases such as vascular endothelial growth factor receptor (VEGFR) and platelet-derived growth factor receptor (PDGFR) [7]. Sorafenib has shown potent antitumor activity in vitro and in vivo in a broad range of malignancies including renal cell, hepatocellular, breast, colon, pancreas, and ovarian carcinomas [8, 9]. On the basis of the results of the SHARP study [10], sorafenib was approved for treatment of unresectable hepatocellular carcinoma (HCC) cases. A phase II trial of single-agent sorafenib in patients with advanced biliary tract carcinoma has been conducted [11]. In addition, sorafenib was recently reported to exert in vitro antitumor activity against human cholangiocarcinoma through blockage of growth factor-induced activation of the mitogen-activated protein kinase (MAPK) pathway and cell cycle arrest [12]. Sorafenib therefore merits further in vitro and in vivo evaluations to explore the mechanisms and molecular pathways involved in the observed antitumor activity in a panel of human ICC cell lines.

In this study, the in vitro and in vivo tumor activity of sorafenib was assessed in preclinical models using human ICC cell lines with focus on (1) the molecular mechanisms responsible for the observed tumor growth inhibition and apoptosis induction and (2) whether ICC is targeted in vivo in animals bearing subcutaneously (s.c.) growing xenografted tumors or peritoneally disseminated ICC tumors. Treatment with sorafenib resulted in inhibition of MEK and MAPK phosphorylation as well as interleukin-6-induced phosphorylation of signal transducer and activator of transcription 3 (STAT3) in ICC cells. Down-regulation of the anti-apoptotic protein myeloid cell leukemia-1 (Mcl-1) paralleled the reduced phosphorylation of STAT3. Administration of a tolerable dose of sorafenib induced significant regression of established ICC tumors and significantly improved the survival of animals with disseminated tumors.

Materials and methods

Cell line and animals

The experiments were performed on 8 human ICC cell lines: YSCCC and HuH-28 from RIKEN Cell Bank (Ibaraki, Japan), HuCCT-1 from the Health Science Research Resources Bank (Osaka, Japan), KMC-1 and KMCH-1 [13, 14] from Dr. M. Kojiro (Kurume University School of Medicine, Kurume, Japan), CCKS-1 [15] from

Dr. Y. Nakanuma (Kanazawa University Graduate School, Kanazawa, Japan), and KKU-100 and KKU-M214 [16, 17] from Dr. B. Sripa (Khon Kaen University, Thailand). In addition, PLC/PRF/5, a human hepatocellular carcinoma cell line, was obtained from the American Type Culture Collection (Rockville, MD). CCKS-1 cells were cultured in RPMI 1640 medium and other cell lines were cultured in Dulbecco's modified Eagle's medium (DMEM) containing 10% heat-inactivated fetal calf serum (Invitrogen, Carlsbad, CA, USA) in a humidified atmosphere with 5% CO_2 at 37°C. To establish KKU-100 cells expressing luciferase (KKU-100-luc), an *Xho*I–*Bam*HI fragment containing a full-length luciferase cDNA was inserted into the corresponding site of GCDNsamIRES/EGFP [18], which was referred to as pGCDNsamLucI/E. The vector was converted to the corresponding retrovirus by transduction into 293gpg as described elsewhere [19]. KKU-100 cells were infected with retrovirus GCDNsamLucI/E. The expression level of luciferase was confirmed by using a luciferase assay reagent (Promega, Madison, WI, USA). Four-week-old female BALB/c nu/nu athymic mice were purchased from Sankyo Labo Service (Tokyo, Japan). All animal experiments were approved by the Institutional Animal Care and Use Committee of Tokyo Women's Medical University.

Sorafenib (Nexavar™)

Sorafenib tosylate was provided by Bayer Schering Pharma (Leverkusen, Germany). For in vitro administration, sorafenib was dissolved in dimethyl sulfoxide (DMSO) to a concentration of 10 mmol/L and further diluted to an appropriate final concentration in fresh media. In all experiments, the final DMSO concentration did not exceed 0.1%, thus not affecting cell growth. For in vivo administration, sorafenib was dissolved in Cremophor EL/ethanol (50:50; Sigma Cremophor EL, 95% ethanol) and handled as described previously [7].

Cell viability assay

The in vitro effect of sorafenib on growth inhibition of ICC cell lines was determined by a cell viability assay using a WST-8 reduction assay kit (Dojin Laboratories, Tokyo, Japan) according to the manufacturer's instructions. Cells were plated at 5,000 per well in 96-well microtiter plates and incubated overnight. On the following day, various concentrations of sorafenib were added to the wells and the cells were incubated for an additional 72 h. WST-8 was added and cell viability was determined by reading optical density values from a microplate reader at an absorption wavelength of 450 nm. All assays were performed twice. The IC_{50} value, at which 50% cell growth inhibition compared with that of the DMSO control was obtained, was calculated.

Annexin V apoptosis assay

Cells were cultured in 6-well plates at 3×10^5 cells per well. On the following day, the cells were treated with sorafenib at concentrations of 0, 5, 10, and 15 μmol/L for 24 or 48 h. After the treatment, both detached and attached cells were collected and apoptotic cells were detected by using an Annexin V-FITC Apoptosis Detection Kit (Beckman Coulter). The cells were stained with Annexin V-FITC and propidium iodide (PI) according to the manufacturer's instructions. The apoptotic fraction was identified as Annexin V-positive and PI-negative cells using a FACS Calibur (Becton–Dickinson, San Jose, CA, USA). All assays were performed in quadruplicate.

Terminal dUTP nick-end labeling (TUNEL) assay

Cells were cultured on chamber slides and allowed to adhere overnight, and they were then treated with sorafenib at concentrations of 0, 5, 10, and 15 μmol/L for 24 h. Apoptosis of the cells was evaluated on the basis of the TUNEL assay using the Dead End Fluorometric TUNEL System (Promega, Madison, WI, USA) according to the manufacturer's instructions. All assays were performed in quadruplicate.

Cell cycle analysis

Cells were cultured in 6-well plates at 3×10^5 cells per well. On the following day, the cells were treated with sorafenib at concentrations of 0, 3, 10, and 15 μmol/L for 24 h. After the treatment, the cell nuclei were isolated using CycleTest PLUS DNA Reagent Kit (Becton–Dickinson). The DNA was stained with PI according to the manufacturer's instructions. The stained DNA was analyzed by a FACS Calibur and the DNA content was quantified using ModFit software (Verity Software House, Topsham, ME, USA). All assays were performed in quadruplicate.

Immunoblot analysis

After treatment, whole-cell lysates were prepared as previously described [20]. Aliquots of cell lysate were loaded on 4–12% gradient sodium dodecyl sulfate polyacrylamide gel electrophoresis (SDS-PAGE) gel, electrophoresed under reducing conditions, and transferred onto a poly(vinylidene difluoride) (PVDF) membrane. Blots were probed with an antibody raised against MAPK, phospho-MAPK (Erk1/2) (Thr^{202}/Tyr^{204}), MEK, phospho-MEK

(Ser^{221}), STAT3, phospho-STAT3 (Tyr^{705}), AKT, phospho-AKT (Ser^{473}), Mcl-1, Bcl-xl, caspase-3, cyclin-dependent kinase inhibitor p27^{kip1} (Cell Signaling Technology Inc, Beverly, MA, USA), cyclin-dependent kinase cyclin D1 (Abcam, Cambridge, MA, USA), or β-actin (Sigma-Aldrich, St. Louis, MO, USA). Proteins were visualized on Hyperfilm^{TM} using an ECL/western blotting system (GE Healthcare, Piscataway, NJ, USA) according to the manufacturer's instructions. β-Actin was used as the internal control. In some experiments, KKU-100 and KMCH-1 cells were treated with 5 or 10 μmol/L sorafenib for 24 h. In the last 10 min of the incubation period with the drug, cells were stimulated with IL-6 (10 ng/ml). The cell lysates were prepared in the same way as described above and subjected to immunoblotting for STAT3, pSTAT3, and Mcl-1.

Subcutaneous xenografted ICC tumor model

An s.c. xenografted model injected with KKU-100 cells was prepared as previously described [20]. Sorafenib was administered orally once daily for 21 days at doses of 10, 30, and 100 mg/kg body weight. Treatment was initiated when tumor volumes reached median sizes of 140–180 mm^3 with 8 mice per group. Body weights and tumor volume were measured twice weekly starting on the first day of treatment. Tumor size was measured using Vernier calipers and tumor volume was calculated as 0.5 × longest diameter × width^2. The percentage of tumor inhibition was calculated according to the formula $[1 - (T/C)] \times 100$, where T and C represent the mean tumor volumes of the treatment group and the control group, respectively. In some experiments, animals with tumors measuring 150–300 mm^3 in size were administered sorafenib orally once daily for 5 days at doses of 30 and 100 mg/kg. Tumors were harvested 3 h after the last treatment and either homogenized in lysis buffer for immunoblot analysis or fixed in paraformaldehyde and paraffin-embedded. Immunohistochemical staining of tumors was done with a monoclonal Ab raised against CD31 (Abcam). TUNEL staining for tumor tissue was based on the protocol of the Dead End Colorimetric TUNEL System (Promega). The tissue sections were viewed at ×100 magnification and images were captured with a digital camera. Four fields per section were analyzed, excluding peripheral connective tissue and necrotic regions. Microvessel density (MVD) in each field was defined as the mean number of microvessels containing high levels of CD31-stained microvessels. Percentage of apoptotic cells was defined as TUNEL-positive cells among 1000 tumor cells. Mean values of MVD and percentage of TUNEL-positive cells in each group were calculated from three tumor specimens.

Intraperitoneally disseminated ICC tumor model

An intraperitoneal (i.p.) dissemination model injected with KKU-100-luc cells was prepared as previously described [20]. Five days after tumor cell injection, establishment of intraperitoneally disseminated ICC was confirmed by injection of luciferin and imaging of photon emission. The mice were randomized into 3 groups: vehicle control or daily administration of sorafenib at 10 or 30 mg/kg with 8 mice per group. Mice were weighed twice weekly and killed if they had lost more than 20% of body weight or seemed moribund. The mice were treated for 46 days, and photon counting was conducted one or two times a week. Bioluminescence images were used to monitor the dynamics of peritoneal tumor growth. Immediately before imaging, 150 mg/kg of D-luciferin (Alameda, CA, USA) was administered to mice by i.p. injection. After 15 min, photons from whole bodies were counted using the IVIS imaging system (Xenogen) in accordance with the manufacturer's instructions. Total flux (photons/s) of emitted light was used as a measure of the relative number of viable tumor cells in the peritoneal tumor. Data were analyzed using Living Image 3.0 software (Xenogen).

Statistical analysis

Values are given as mean ± SD (standard deviation). Statistical evaluations of data were analyzed using one-way analysis of variance (ANOVA) followed by the Tukey–Kramer test. The survival of animals in the peritoneal dissemination model was analyzed using the Kaplan–Meier method. Differences in the survival of animals in subgroups were analyzed by the log-rank test. A P value of less than 0.05 was defined as statistically significant.

Results

Sorafenib inhibits proliferation of ICC cells

Treatment of ICC cells with sorafenib for 72 h resulted in potent growth inhibition in a dose-dependent manner for all of the 8 cell lines studied (Fig. 1). The IC_{50} of sorafenib ranged from 3.8 to 10.3 μmol/L. KKU-100 was found to be most sensitive and HuH-28 least sensitive to the drug. In terms of the IC_{50} value, five of the 8 ICC cell lines studied were comparable to PLC/PRF/5, a human HCC cell line (IC_{50} 7.0 ± 0.3 μmol/L).

Sorafenib induces apoptosis in ICC cells

Four ICC cell lines, KKU-100, KMCH-1, HuCCT-1, and CCKS-1, were treated with sorafenib at concentrations of

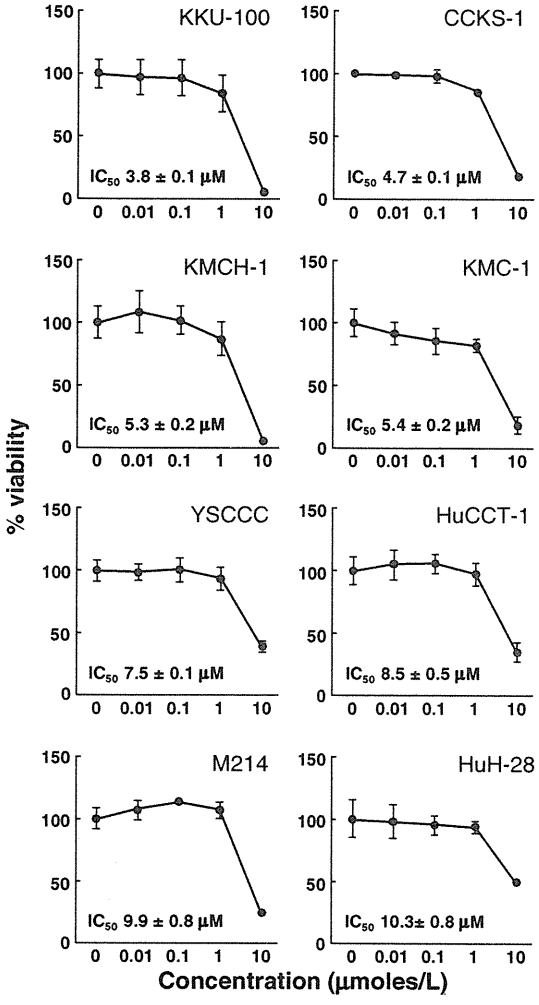

Fig. 1 In vitro growth inhibition of ICC cells cultured with sorafenib. Eight ICC cell lines (5×10^3 cells) were cultured in DMEM or RPMI 1640 medium with various concentrations of sorafenib (0–10 μmol/L) for 72 h at 37°C. Growth inhibition data are given as percentages of the viability of cells cultured without the drug. The results are presented as mean ± SD of sextuplicate determinations. The assay was repeated twice

5, 10, and 15 μmol/L for 24 and 48 h. In flow cytometry analysis, the proportion of annexin V-positive and PI-negative cells was increased in a dose-dependent and time-dependent manner for all of the 4 ICC cell lines studied (Fig. 2a). Similar to the results of flow cytometry analysis, in the TUNEL assay (Figs. 2b, c), the percentages of TUNEL-positive cells in the 4 ICC cell lines were 1.9–3.8% without treatment and 4–8% with 5 μmol/L, 8–12% with 10 μmol/L, and 10–17% with 15 μmol/L sorafenib treatment for 24 h.

Sorafenib induces no cell cycle arrest

Three ICC cell lines, KKU-100, KMCH-1, and HuCCT-1, were treated with sorafenib at concentrations of 3, 10, and 15 μmol/L for 24 h. The cell cycle analysis by flow cytometry showed that the sorafenib treatment for 24 h did not cause any significant changes in the cell cycle distribution in these cells (Fig. 3). The cell cycle arrest, that is, the increase in the G_1 phase and the decrease in the S phase, was not observed in these cells (Fig. 3a). Supporting this observation, the immunoblot analysis revealed that the treatment did not induce any changes in the expression levels of the cell cycle promoter cyclin D1 and the cell cycle inhibitor $p27^{Kip1}$ (Fig. 3b), both of which are important for cell cycle regulation [21, 22].

Sorafenib inhibits the RAF/MEK/MAPK signaling pathway in ICC cells

Following the observation that sorafenib inhibits the RAF/MEK/MAPK signaling pathway in a number of tumors, this inhibitory effect of the drug was investigated for 2 ICC cell lines, KKU-100 and KMCH-1. By treatment at concentrations of 2.5–10 μmol/L, hyperphosphorylation of MEK and MAPK was inhibited in these cells (Fig. 4a). However, hyperphosphorylation of AKT, a signaling molecule on the PI3 kinase pathway, was not inhibited (Fig. 4a).

Sorafenib reduces STAT3 and Mcl-1 expression levels

In human cholangiocarcinoma cells, sorafenib was recently shown to inhibit the JAK/STAT3 signaling axis at the level of STAT3 phosphorylation, leading to down-regulation of Mcl-1, an anti-apoptotic protein [23]. Therefore, this inhibitory effect of the drug was investigated for KKU-100 and KMCH-1 cells. By treatment at concentrations of 2.5–10 μmol/L, hyperphosphorylation of STAT3 was inhibited in these cells (Fig. 4b). Expression of the anti-apoptotic protein Mcl-1, but not that of Bcl-xL, was potently down-regulated in the cells (Fig. 4b). Moreover, cleavage of caspase-3, which is reportedly found in apoptotic cells, was detected in cells treated at a concentration of 10 μmol/L. These results are consistent with the induction of apoptosis by sorafenib through a down-regulation of Mcl-1, which may be independent of the inhibitory effects on MEK/MAPK signaling. As shown in Fig. 4c, in KKU-100 and KMCH-1 cells, interleukin-6 (IL-6)-stimulated phosphorylation of STAT3 was inhibited by sorafenib at a concentration of 10 μmol/L. Sorafenib also decreased Mcl-1 levels in the presence of IL-6 (Fig. 4c). Because the IL-6/STAT3 pathway is known to control Mcl-1 transcription in human ICC [24], the inhibition of IL-6-induced STAT3 activation by sorafenib may be one mechanism by which sorafenib exerts potent antitumor activity against human ICC cells.

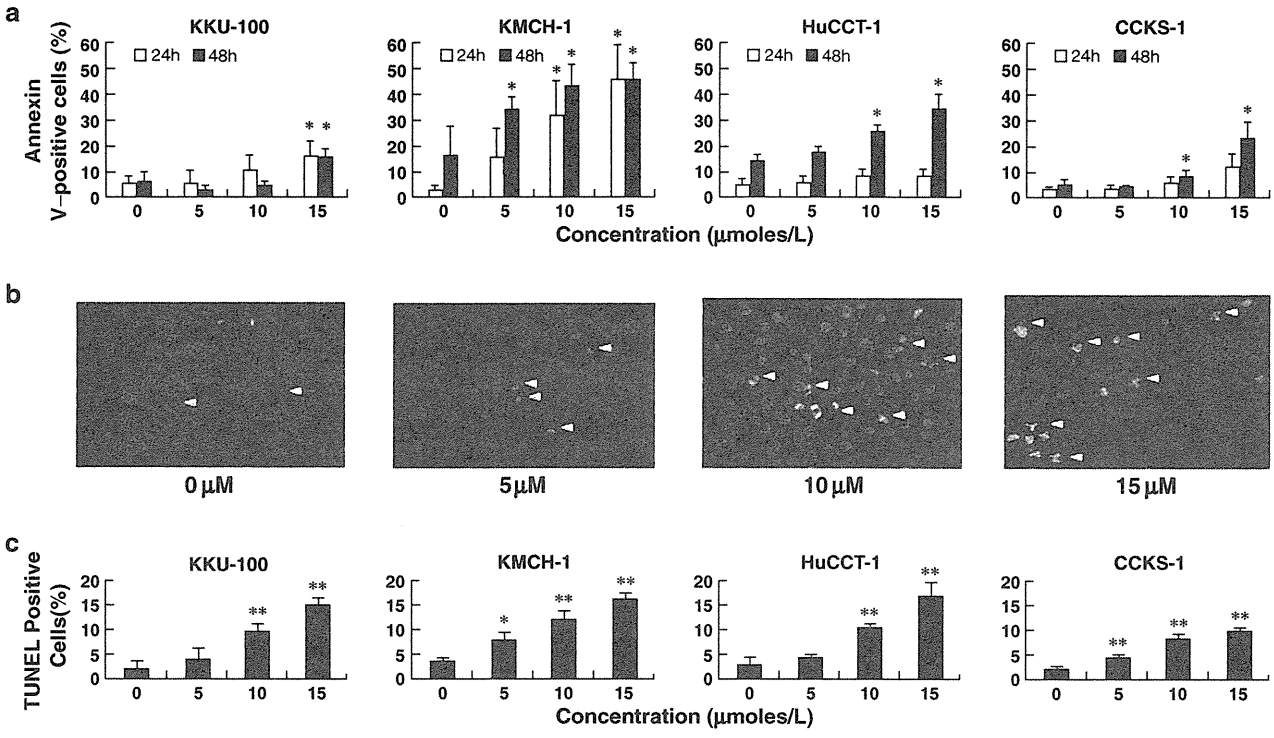

Fig. 2 Induction of apoptosis in ICC cells by sorafenib. **a** ICC cells were treated with various concentrations of sorafenib (0–15 μmol/L) for 24 and 48 h at 37°C. The apoptotic fraction identified as Annexin V-positive and PI-negative cells was determined by flow cytometric analysis. **b** TUNEL staining was done for ICC cells (KKU-100, KMCH-1, HuCCT-1, and CCKS-1 cells) treated with sorafenib for 24 h. *Green* nuclear staining indicates apoptotic cells. **c** The percentage of TUNEL-positive cells was quantified for each cell line. *Columns* and *error bars* represent means of three independent determinations and SD, respectively. Significant differences between the DMSO controls and the treatment groups are indicated by $*P < 0.05$ or $**P < 0.01$. All assays were performed in quadruplicate

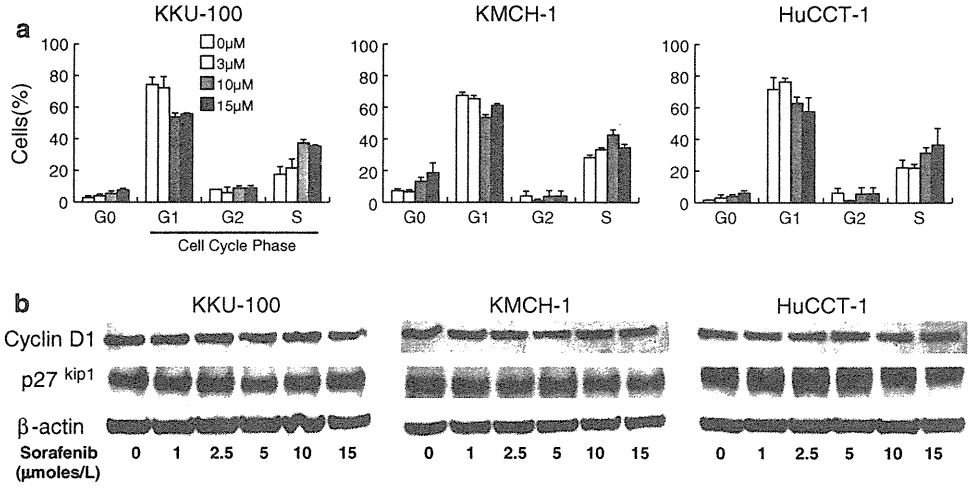

Fig. 3 Effects of sorafenib on cell cycle distribution in ICC cells (KKU-100, KMCH-1, and HuCCT-1). **a** ICC cells were treated with various concentrations of sorafenib (0–15 μmol/L) for 24 h at 37°C. After the treatment, the cell nuclei were isolated and stained with PI. The stained DNA was analyzed by flow cytometry, and then the DNA content was quantified. **b** Immunoblot analysis of cell cycle promoter cyclin D1 and the cell cycle inhibitor $p27^{Kip1}$ in the cells. The cells were treated with various concentrations of sorafenib (0–15 μmol/L) for 24 h

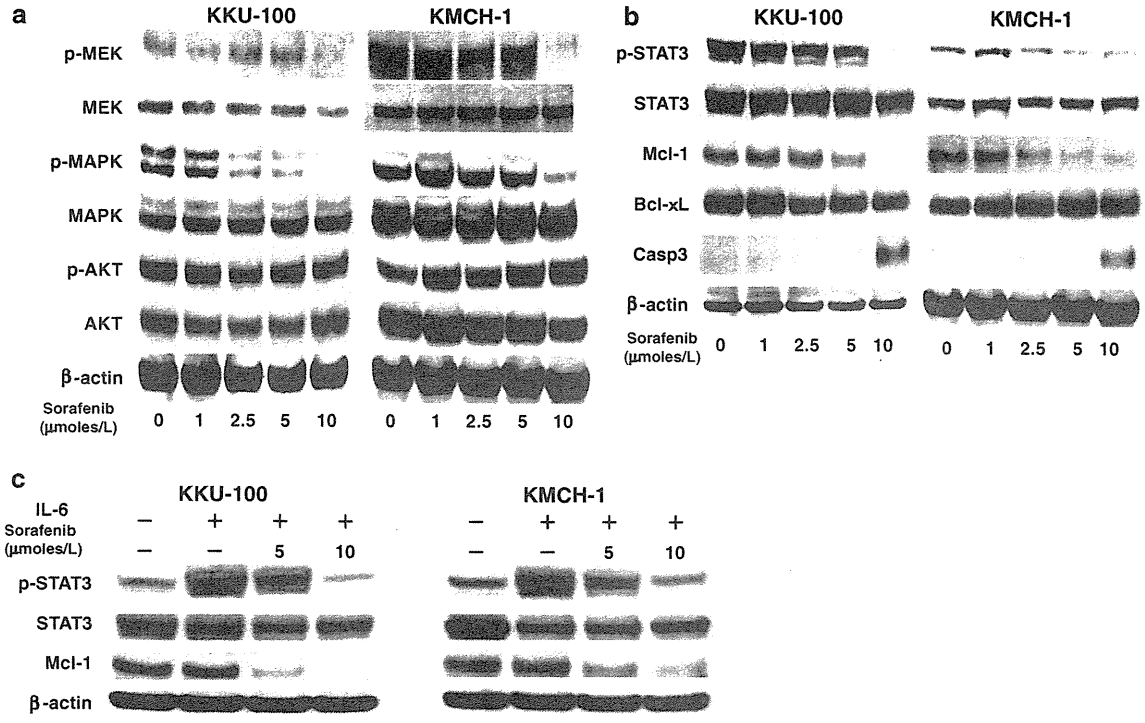

Fig. 4 Effects of sorafenib on expression of cell signaling molecules and apoptosis-related molecules in ICC cells (KKU-100 and KMCH-1 cells). **a** Immunoblot analysis of cell signaling molecules, MEK, MAPK, and Akt. The cells were treated with various concentrations of sorafenib (0–10 μmol/L) for 4 h. **b** Immunoblot analysis of cell signaling molecule STAT3 and apoptosis-related molecules, Mcl-1, Bcl-xL, and cleaved caspase-3, in the cells. The cells were treated with various concentrations of sorafenib (0–10 μmol/L) for 24 h. **c** Immunoblot analysis of STAT3 and Mcl-1 in the cells with and without IL-6 stimulation in the sorafenib treatment. The cells were treated with various concentrations of sorafenib (0–10 μmol/L) for 24 h and then stimulated with IL-6 for 10 min. Each protein was normalized to β-actin

In vivo antitumor activity of sorafenib against s.c. xenografted ICC tumors

Following the observation of potent antitumor activity in vitro, the in vivo antitumor activity of sorafenib was studied using s.c. tumor-bearing mice. As shown in Fig. 5a, sorafenib inhibited growth of s.c. xenografted tumors at all doses tested. Compared with the vehicle-treated group, mice treated with 10, 30, and 100 mg/kg sorafenib showed 44, 75, and 84% inhibition of tumor growth on day 16 after the start of treatment, respectively ($P < 0.001$). No evidence of toxicity, as determined by increased weight loss relative to control animals or drug-related lethality, was observed in any of the groups. As shown in Fig. 5b, in the s.c. xenografted tumors of mice treated with sorafenib, the expression levels of pMAPK and pSTAT3 and that of Mcl-1 were decreased, whereas the level of cleaved caspase-3 was increased. Moreover, MVD was significantly decreased in tumor specimens from sorafenib-treated groups compared with that in specimens from the vehicle-treated group, as assessed by CD31 staining (Fig. 5c). Figure 5c also shows that sorafenib induced tumor cell apoptosis as measured by TUNEL staining at both doses evaluated. The reduction in MVD and increase in TUNEL-positive staining are quantified in graphs shown in Fig. 5d. MVD was reduced from 28.8 counts/field in the vehicle-treated group to 11.3 and 5 counts/field in the groups treated with 30 and 100 mg/kg sorafenib, respectively. TUNEL staining in the same samples was increased from 1.7% positive area in the vehicle-treated group to 8.7 and 11.6% positive areas in the groups treated with 30 and 100 mg/kg sorafenib, respectively.

In vivo antitumor activity of sorafenib against peritoneally disseminated ICC tumors

To mimic the clinical aggressiveness of ICC, a peritoneally disseminated tumor model was developed using immunodeficient mice that were inoculated with KKU-100-luc cells into the peritoneal cavity. Five days after cell implantation, establishment of peritoneally disseminated ICC was confirmed using IVIS (Fig. 6a). After administration of sorafenib, tumor volume in the intraperitoneal cavity was assessed using the IVIS imaging system that visualizes viable tumor cells as photon intensity (Fig. 6b). The intensity of light-emitting signals is depicted according

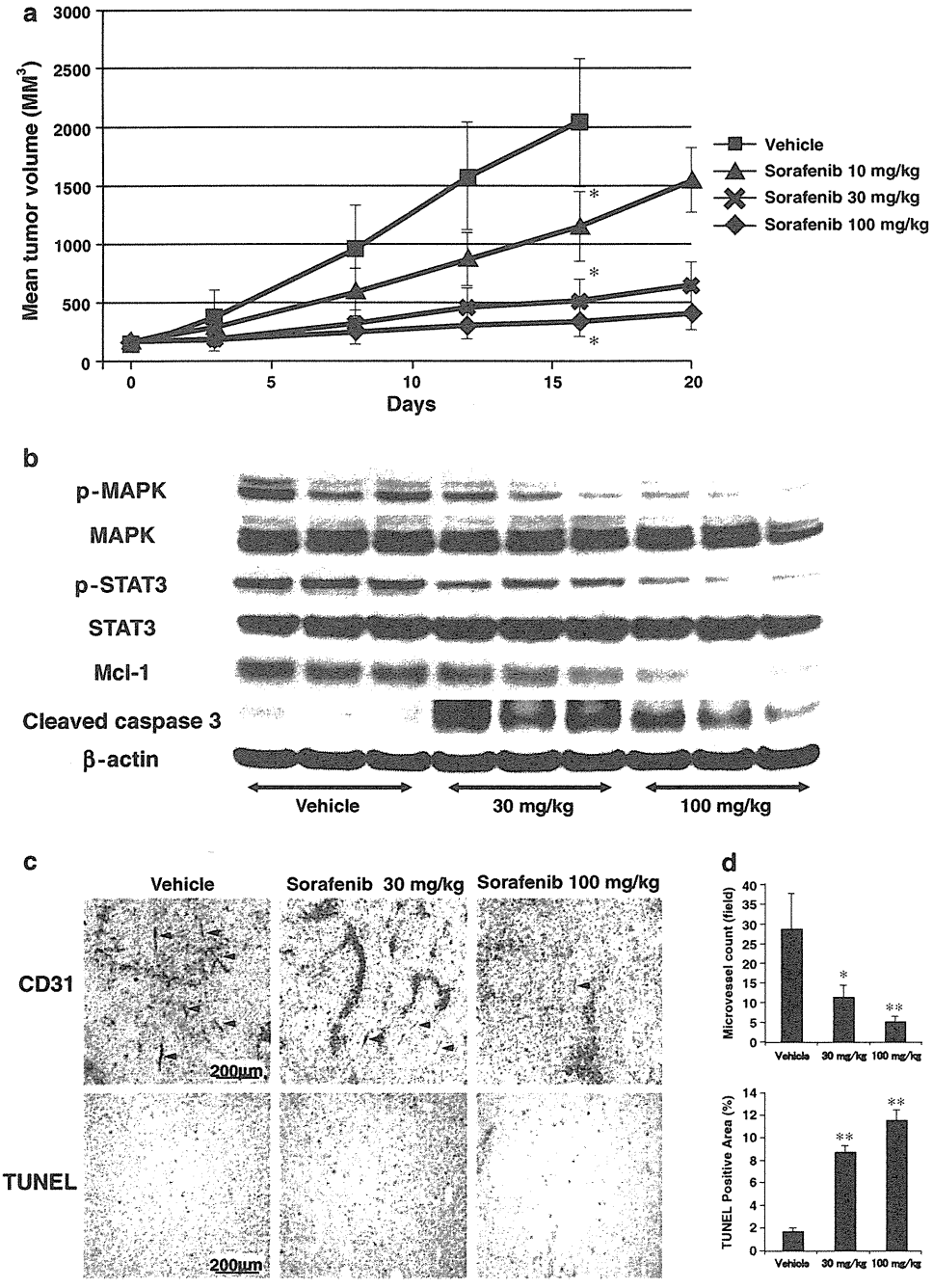

Fig. 5 In vivo antitumor activity of sorafenib against s.c. xenografted tumors of ICC cells in mice. **a** Subcutaneous tumors were seeded in immunodeficient mice using KKU-100 cells, as described in the "Materials and methods". Each group consisted of 8 animals. Tumor volumes were measured two or three times a week, and tumor volume (mm^3) was calculated as 0.5 × longest diameter × width^2. Tumor volumes are presented as mean ± SD of 8 mice for each group. The mice in vehicle-treated group had to be euthanized on day 16 due to tumor burden. Significant differences between the treatment groups and vehicle-treated group are indicated by $^*P < 0.01$. A significant reduction in tumor volume was observed in a dose-dependent manner in mice in the sorafenib groups 16 days after the start of treatment. **b** Immunoblot analysis of MAPK, STAT3, Mcl-1, and cleaved caspase-3 in the tumors. Each protein was normalized to β-actin. Tumor samples from 3 representative animals from each group are shown. **c** CD31 staining and TUNEL staining in the tumors. **d** Quantification of microvessel (assessed by CD31 staining) and TUNEL-positive cells from immunohistochemical analysis of the tumors. *Columns* and *error bars* represent means and SD of the values of MVD and those of TUNEL-positive cells in each group, respectively. Significant differences between the treatment groups and vehicle-treated group are indicated by $^*P < 0.05$ or $^{**}P < 0.01$

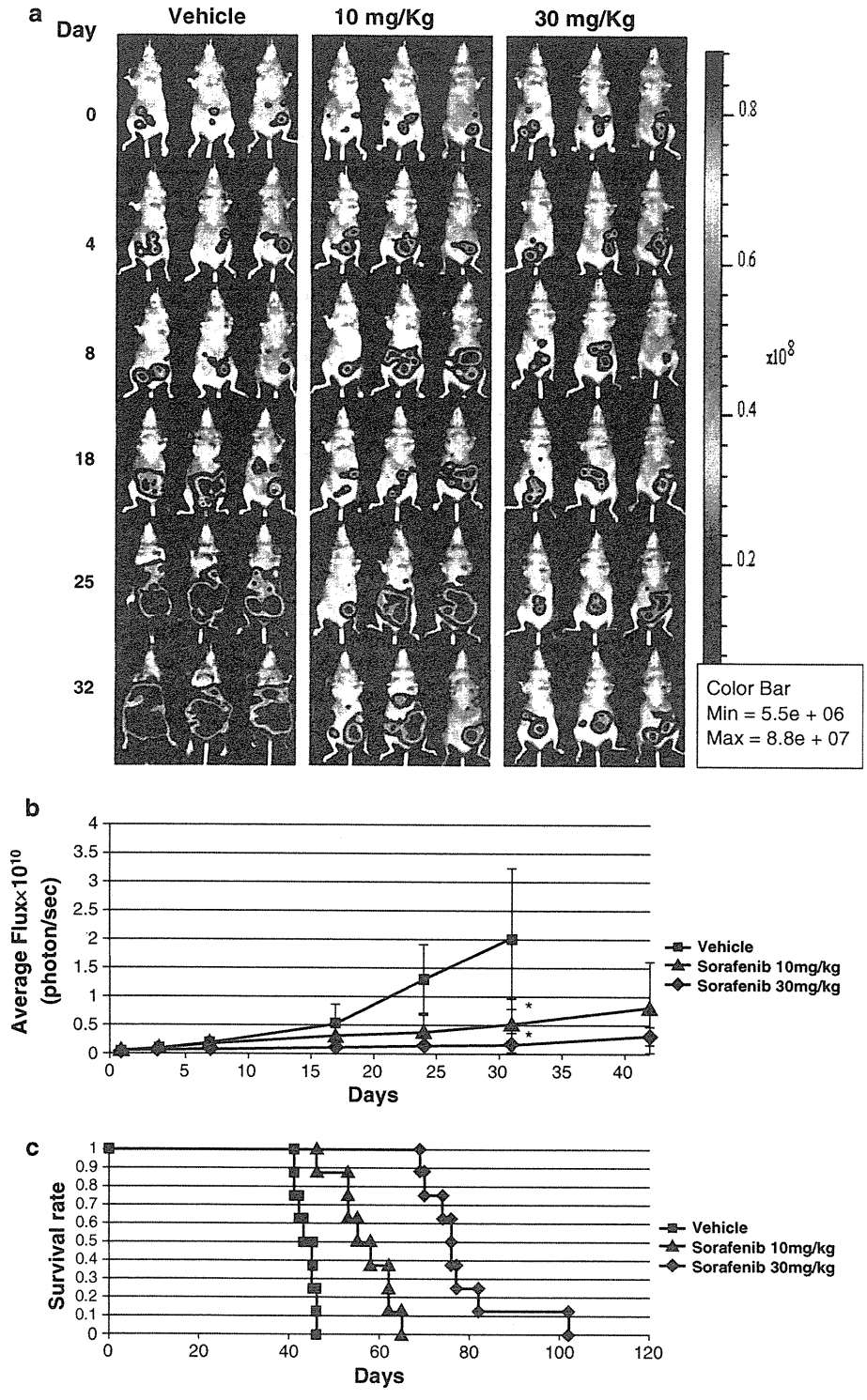

Fig. 6 In vivo antitumor activity of sorafenib against peritoneally disseminated tumors of ICC cells in mice. Peritoneally disseminated tumors were seeded in immunodeficient mice using KKU-100-luc cells (5×10^6 cells/mouse), as described in the "Materials and methods". Each group consisted of 8 animals. **a** Sequential in vivo whole-body imaging of tumor progression over time. Bioluminescence images facilitated real-time visualization of tumor burden in live animals. *Panels* depict three representative mice from each of the vehicle- and sorafenib-treated (10 and 30 mg/kg body weight) groups. Images were captured every other day after the treatment started. **b** Time course of changes in quantification of tumor bioluminescence. *Points* represent the mean area of bioluminescence for live intact animals in each treatment group ($n = 8$ mice); *error bars*, SD. Significant differences between the treatment groups and vehicle-treated group are indicated by $*P < 0.01$. **c** Relationship between survival outcome and sorafenib treatment in mice with peritoneally disseminated tumors of ICC cells as assessed using Kaplan–Meier survival curves. The median survival period in the vehicle group was 43 days, and the mean survival periods in the groups treated with sorafenib at doses of 10 and 30 mg/kg body weight were 55 and 76 days, respectively. The difference was statistically significant ($P < 0.005$)

to the color bar in Fig. 6a. The blue area indicates small amounts of tumor, whereas the red area indicates large amounts of tumor. In stark contrast to the vehicle group where the intensity and area of light emission increased over time, those of the 10 and 30 mg/kg sorafenib-treated groups decreased over time. On day 31 after the start of treatment, the average photon intensity (total flux) was significantly decreased in the treated groups compared with that in the vehicle-treated group ($P < 0.001$). In addition, as shown in Fig. 6c, the median survival periods in the treated groups at doses of 10 and 30 mg/kg were 55 and 76 days, respectively, which were significantly longer than the survival period of 43 days in the vehicle-treated group ($P < 0.005$).

Discussion

Therapeutic options for ICC are unsatisfactory, and the survival outcome is therefore poor. Effective therapeutic approaches against this aggressive disease are urgently needed. Sorafenib was recently approved for treatment of advanced HCC on the basis of positive results of a large phase III randomized clinical trial [10]. Following the positive results for treatment of HCC, the efficacy of this drug against human ICC, a more aggressive disease, was evaluated in preclinical models in this study.

We demonstrated in the human ICC cell lines that sorafenib blocks phosphorylation of MEK/MAPK, and IL-6-stimulated phosphorylation of STAT3, causes down-regulation of Mcl-1, inhibits tumor cell proliferation, and induces apoptosis in vitro. However, in stark contrast to the result of a recent study [12], sorafenib-induced cell cycle arrest (i.e., arrest in the G_1 phase) was not seen in any of the human ICC cell lines that we utilized in this study, in which induction of expression of the cell cycle inhibitor $p27^{Kip1}$ and suppression of the cell cycle promoter cyclin D1 were not observed. Consistent with the observation in this study, a previous study [12, 25] reported that sorafenib-induced cell cycle arrest was not seen in PLC/PRF/5, a human HCC cell line, and EGI-1, a human ICC cell line. Nevertheless, sorafenib exhibited robust in vivo antitumor efficacy, including partial tumor regressions in both an s.c. xenografted tumor model and a peritoneally disseminated tumor model. Moreover, in animals treated with sorafenib, a significant reduction in MVD (tumor angiogenesis) measured by CD31 staining was observed in s.c. xenografted tumors. Collectively, these results provide evidence that sorafenib may be an attractive agent for treatment of ICC by simultaneously inhibiting both tumor angiogenesis (VEGF and PDGF signaling) and tumor cell survival (RAF kinase signaling-dependent and STAT3 signaling-dependent mechanisms) rather than by inducing tumor cell cycle arrest.

In ICC, inflammation-associated carcinogenesis is, in part, mediated by dysregulated cytokine signaling pathways [26], which potentially can be therapeutically targeted for treatment of this cancer. Members of the STAT family are key signal transducers in cytokine and growth factor signaling. STAT3 has been shown to be an essential signaling molecule in cholangiocarcinogenesis through its transcriptional activity on genes regulating apoptosis, proliferation, differentiation, and angiogenesis [27, 28]. One of the main activators of STAT3 in ICC cells is IL-6 via JAK [29]. IL-6 is a cytokine secreted by inflammatory cells (i.e., macrophages) but also by ICC cells, where it activates STAT3 by autocrine and paracrine mechanisms [24, 30–32]. Activation of STAT3 transcriptionally targets Mcl-1, an anti-apoptotic Bcl-2 family protein [24]. The results of this study support results recently reported by Blechacz et al. [23] showing that sorafenib inhibits the JAK/STAT3 signaling axis at the level of STAT3 phosphorylation, resulting in down-regulation of Mcl-1, thereby sensitizing human ICC cells to apoptosis.

Sorafenib exhibited significant antitumor activity against ICC tumors in the peritoneal metastasis model. In the clinical course of ICC, peritoneal dissemination is a very unfavorable development that frequently occurs in patients with advanced ICC. Since systemic chemotherapy using anticancer drugs has shown few significant benefits for patients with advanced ICC (e.g., peritoneally disseminated ICC) [33, 34], administration of sorafenib may be a useful option.

In summary, this study showed that sorafenib induces inhibition of the RAF/MEK/MAPK signaling pathway, reduction of STAT3 phosphorylation, and down-regulation of Mcl-1 protein level, all of which may contribute to the pro-apoptotic effects of the drug and also to the pronounced antivascular effects in in vitro and in vivo models using human ICC cells. A recent preclinical study provided a rationale for sorafenib's suitability for combination therapy with chemotherapeutic agents [12]. The results of this study may provide a rationale for a monotherapeutic approach against ICC by sorafenib or for the use of sorafenib in combination with other chemotherapeutic agents, and the results indicate the need for a phase II or III clinical trial.

Acknowledgments This work was supported in part by Grants-in-Aid for Scientific Research from the Ministry of Education, Culture, Sports, Science and Technology, Japan (20390339, 22390379, 22591530).

Conflict of interest All authors declare that they have no conflict of interests or financial interests.

References

1. Blechacz B, Gores GJ. Cholangiocarcinoma: advances in pathogenesis, diagnosis, and treatment. Hepatology. 2008;48:308–21.
2. Khan SA, Thomas HC, Davidson BR, Taylor-Robinson SD. Cholangiocarcinoma. Lancet. 2005;366:1303–14.
3. Lazaridis KN, Gores GJ. Cholangiocarcinoma. Gastroenterology. 2005;128:1655–67.
4. Jarnagin WR, Fong Y, DeMatteo RP, Gonen M, Burke EC, Bodniewicz BJ, et al. Staging, resectability, and outcome in 225 patients with hilar cholangiocarcinoma. Ann Surg. 2001;234:507–17 (discussion 517–9).
5. Huang JL, Biehl TR, Lee FT, Zimmer PW, Ryan JA Jr. Outcomes after resection of cholangiocellular carcinoma. Am J Surg. 2004;187:612–7.
6. Tabernero J. The role of VEGF and EGFR inhibition: implications for combining anti-VEGF and anti-EGFR agents. Mol Cancer Res. 2007;5:203–20.
7. Wilhelm SM, Carter C, Tang L, Wilkie D, McNabola A, Rong H, et al. BAY 43–9006 exhibits broad spectrum oral antitumor

activity and targets the RAF/MEK/ERK pathway and receptor tyrosine kinases involved in tumor progression and angiogenesis. Cancer Res. 2004;64:7099–109.
8. Wilhelm SM, Adnane L, Newell P, Villanueva A, Llovet JM, Lynch M. Preclinical overview of sorafenib, a multikinase inhibitor that targets both Raf and VEGF and PDGF receptor tyrosine kinase signaling. Mol Cancer Ther. 2008;7:3129–40.
9. Strumberg D, Richly H, Hilger RA, Schleucher N, Korfee S, Tewes M, et al. Phase I clinical and pharmacokinetic study of the Novel Raf kinase and vascular endothelial growth factor receptor inhibitor BAY 43-9006 in patients with advanced refractory solid tumors. J Clin Oncol. 2005;23:965–72.
10. Llovet JM, Ricci S, Mazzaferro V, Hilgard P, Gane E, Blanc JF, et al. Sorafenib in advanced hepatocellular carcinoma. N Engl J Med. 2008;359:378–90.
11. Bengala C, Bertolini F, Malavasi N, Boni C, Aitini E, Dealis C, et al. Sorafenib in patients with advanced biliary tract carcinoma: a phase II trial. Br J Cancer. 2010;102:68–72.
12. Huether A, Hopfner M, Baradari V, Schuppan D, Scherubl H. Sorafenib alone or as combination therapy for growth control of cholangiocarcinoma. Biochem Pharmacol. 2007;73:1308–17.
13. Iemura A, Maruiwa M, Yano H, Kojiro M. A new human cholangiocellular carcinoma cell line (KMC-1). J Hepatol. 1992;15: 288–98.
14. Murakami T, Yano H, Maruiwa M, Sugihara S, Kojiro M. Establishment and characterization of a human combined hepatocholangiocarcinoma cell line and its heterologous transplantation in nude mice. Hepatology. 1987;7:551–6.
15. Saito K, Minato H, Kono N, Nakanuma Y, Ishida F, Kosugi M. Establishment of the human cholangiocellular carcinoma cell line (CCKS1). Kanzo. 1993;34:122–9 (in Japanese).
16. Sripa B, Leungwattanawanit S, Nitta T, Wongkham C, Bhudhisawasdi V, Puapairoj A, et al. Establishment and characterization of an opisthorchiasis-associated cholangiocarcinoma cell line (KKU-100). World J Gastroenterol. 2005;11:3392–7.
17. Tepsiri N, Chaturat L, Sripa B, Namwat W, Wongkham S, Bhudhisawasdi V, et al. Drug sensitivity and drug resistance profiles of human intrahepatic cholangiocarcinoma cell lines. World J Gastroenterol. 2005;11:2748–53.
18. Nabekura T, Otsu M, Nagasawa T, Nakauchi H, Onodera M. Potent vaccine therapy with dendritic cells genetically modified by the gene-silencing-resistant retroviral vector GCDNsap. Mol Ther. 2006;13:301–9.
19. Suzuki A, Obi K, Urabe T, Hayakawa H, Yamada M, Kaneko S, et al. Feasibility of ex vivo gene therapy for neurological disorders using the new retroviral vector GCDNsap packaged in the vesicular stomatitis virus G protein. J Neurochem. 2002;82: 953–60.
20. Ishige K, Shoda J, Kawamoto T, Matsuda S, Ueda T, Hyodo I, et al. Potent in vitro and in vivo antitumor activity of interleukin-4-conjugated Pseudomonas exotoxin against human biliary tract carcinoma. Int J Cancer. 2008;123:2915–22.
21. Hirai H, Roussel MF, Kato JY, Ashmun RA, Sherr CJ. Novel INK4 proteins, p19 and p18, are specific inhibitors of the cyclin D-dependent kinases CDK4 and CDK6. Mol Cell Biol. 1995;15: 2672–81.
22. Kato JY, Matsuoka M, Polyak K, Massague J, Sherr CJ. Cyclic AMP-induced G1 phase arrest mediated by an inhibitor (p27Kip1) of cyclin-dependent kinase 4 activation. Cell. 1994; 79:487–96.
23. Blechacz BR, Smoot RL, Bronk SF, Werneburg NW, Sirica AE, Gores GJ. Sorafenib inhibits signal transducer and activator of transcription-3 signaling in cholangiocarcinoma cells by activating the phosphatase shatterproof 2. Hepatology. 2009;50:1861–70.
24. Isomoto H, Kobayashi S, Werneburg NW, Bronk SF, Guicciardi ME, Frank DA, et al. Interleukin 6 upregulates myeloid cell leukemia-1 expression through a STAT3 pathway in cholangiocarcinoma cells. Hepatology. 2005;42:1329–38.
25. Liu L, Cao Y, Chen C, Zhang X, McNabola A, Wilkie D, et al. Sorafenib blocks the RAF/MEK/ERK pathway, inhibits tumor angiogenesis, and induces tumor cell apoptosis in hepatocellular carcinoma model PLC/PRF/5. Cancer Res. 2006;66:11851–8.
26. Yu H, Jove R. The STATs of cancer—new molecular targets come of age. Nat Rev Cancer. 2004;4:97–105.
27. Hirano T, Ishihara K, Hibi M. Roles of STAT3 in mediating the cell growth, differentiation and survival signals relayed through the IL-6 family of cytokine receptors. Oncogene. 2000;19:2548–56.
28. Aggarwal BB, Sethi G, Ahn KS, Sandur SK, Pandey MK, Kunnumakkara AB, et al. Targeting signal-transducer-and-activator-of-transcription-3 for prevention and therapy of cancer: modern target but ancient solution. Ann N Y Acad Sci. 2006;1091: 151–69.
29. Heinrich PC, Behrmann I, Haan S, Hermanns HM, Muller-Newen G, Schaper F. Principles of interleukin (IL)-6-type cytokine signalling and its regulation. Biochem J. 2003;374:1–20.
30. Bollrath J, Phesse TJ, von Burstin VA, Putoczki T, Bennecke M, Bateman T, et al. gp130-mediated Stat3 activation in enterocytes regulates cell survival and cell-cycle progression during colitis-associated tumorigenesis. Cancer Cell. 2009;15:91–102.
31. Grivennikov S, Karin E, Terzic J, Mucida D, Yu GY, Vallabhapurapu S, et al. IL-6 and Stat3 are required for survival of intestinal epithelial cells and development of colitis-associated cancer. Cancer Cell. 2009;15:103–13.
32. Kobayashi S, Werneburg NW, Bronk SF, Kaufmann SH, Gores GJ. Interleukin-6 contributes to Mcl-1 up-regulation and TRAIL resistance via an Akt-signaling pathway in cholangiocarcinoma cells. Gastroenterology. 2005;128:2054–65.
33. Harder J, Riecken B, Kummer O, Lohrmann C, Otto F, Usadel H, et al. Outpatient chemotherapy with gemcitabine and oxaliplatin in patients with biliary tract cancer. Br J Cancer. 2006;95:848–52.
34. Kim ST, Park JO, Lee J, Lee KT, Lee JK, Choi SH, et al. A Phase II study of gemcitabine and cisplatin in advanced biliary tract cancer. Cancer. 2006;106:1339–46.

Infection
DOI 10.1007/s15010-011-0080-1

CASE REPORT

Osteomyelitis due to trimethoprim/sulfamethoxazole-resistant *Edwardsiella tarda* infection in a patient with X-linked chronic granulomatous disease

T. Kawai · H. Kusakabe · A. Seki · S. Kobayashi · M. Onodera

Received: 28 June 2010 / Accepted: 3 January 2011

Abstract *Edwardsiella tarda*, a catalase-positive bacillus widely distributed throughout nature, is generally susceptible to trimethoprim/sulfamethoxazole. We describe osteomyelitis due to trimethoprim/sulfamethoxazole-resistant *E. tarda* in a patient with chronic granulomatous disease (CGD). Once *E. tarda* acquires antibiotic resistance, infected CGD patients may develop severe infections with unforeseeable consequences.

Keywords Chronic granulomatous disease · Immunodeficiency · *Edwardsiella tarda* · Osteomyelitis · Trimethoprim/sulfamethoxazole-resistant

Background

Edwardsiella tarda, which is a gram-negative, catalase-positive bacillus widely distributed throughout nature, has been reported to be a rare pathogen causing gastroenteritis. It also causes severe infections, such as liver abscess, meningitis, cholangitis, and vertebral osteomyelitis [1–4]. Chronic granulomatous disease (CGD) is a rare inherited disorder resulting from the inability of phagocytes to produce bactericidal superoxide anions. CGD patients are highly susceptible to catalase-positive infections, including fungal infections, as well as the development of granulomas in the lungs, liver, kidneys, central nervous system, and bone. Of 203 infections in 23 patients with CGD followed at our center over a 21-year period, the frequency of osteomyelitis was 7%, of lung infections 34%, and of lymphadenitis 15% [5]. *Aspergillus* spp., *Serratia* spp., and *Staphylococcus aureus* were reported as pathogens causing osteomyelitis in patients with CGD [6, 7]. This is the first case report of osteomyelitis caused by trimethoprim/sulfamethoxazole-resistant *E. tarda* infection in a patient with X-linked chronic granulomatous disease (X-CGD).

Case

A 17-year-old boy was diagnosed with X-CGD at the age of 6 months; diagnosis was based on functional analysis showing a failure of phagocytes to produce oxidases. Prophylactic treatment with trimethoprim/sulfamethoxazole has been administrated with interferon gamma therapy after the diagnosis of CGD at the age of 6 months. He has past medical history of liver abscess caused by *S. aureus*, recurrent cervical adenitis, and enteritis, but has not suffered from *E. tarda* previously. The patient's younger brother was also diagnosed with X-CGD, manifesting similar clinical features of recurrent infections. After informed consent was provided, genetic analysis of the patient and his brother identified a mutant version of *c.1381delG* in the *CYBB* gene, corresponding to X-CGD.

T. Kawai · S. Kobayashi · M. Onodera
Department of Human Genetics, National Center for Child Health and Development, Tokyo, Japan

T. Kawai · M. Onodera
Division of Immunology, National Center for Child Health and Development, Tokyo, Japan

H. Kusakabe · A. Seki
Division of Orthopedics, National Center for Child Health and Development, Tokyo, Japan

T. Kawai (✉)
Department of Genetics, National Center for Child Health and Development, 2-10-1 Okura, Setagaya-ku, Tokyo 157-8535, Japan
e-mail: kawai-t@ncchd.go.jp

Published online: 19 January 2011

Upon admission to our center, the patient had a 2-month history of aching pain in his right lower leg, and had developed severe pain with high fever. He had not been treated with antibiotic therapy except for chronic administration of trimethoprim/sulfamethoxazole. Physical examination was unremarkable except for a swollen right lower leg. Hematological assessment revealed leukocytes count 13,800/μl, erythrocyte sedimentation rate 107 mm/h, and C-reactive protein 16.2 mg/dl. Serum (1 → 3)-beta-glucan was slightly elevated to 6.4 pg/ml; however, circulating galactomannan antigen by the Platelia Aspergillus EIA test kit (Bio-Rad Laboratories, Hercules, CA, USA) was less than 0.1 U/ml. Fat-suppressed, gadolinium-enhanced T1-weighted magnetic resonance imaging demonstrated a heterogeneous high-intensity area in the right tibia and significant high signal intensity in the surrounding soft tissue (Fig. 1). Osteomyelitis was diagnosed and treatment was commenced using intravenous meropenem 1 g every 8 h and micafungin 200 mg every 24 h, which targeted both catalase-positive bacteria and fungi that frequently cause osteomyelitis in patients with CGD. Concerned about the worsening of his condition before bone marrow biopsy, we started the treatment immediately after blood culture, urine culture, and hematological assessment including serum (1 → 3)-beta-glucan had been done.

His inflammatory markers gradually reduced until day 6, whereas he continued to have pain in his right lower leg. Because his inflammatory markers elevated again during treatment, an operative procedure employing intramedullary reaming and unroofing was performed on day 7 after the initiation of treatment. Although no microorganisms were isolated from the blood and urine cultures at admission, drainage from the right tibia grew *E. tarda* that, by antimicrobial susceptibility testing, was sensitive to almost all cephem and penicillin antibiotics, and resistant to trimethoprim/sulfamethoxazole. The minimal inhibitory concentration (MIC) of *E. tarda* for trimethoprim/sulfamethoxazole was 152 μg/ml, measured by the BD Phoenix Automated Microbiology System (Becton Dickinson, Sparks, MD, USA) using NMIC/ID30 panels (Becton Dickinson, Sparks, MD, USA) according to the manufacturer's instructions. *E. tarda* was not isolated from stool culture at day 10 after the initiation of treatment. Based on the antimicrobial susceptibility testing, treatment with meropenem and micafungin was replaced with intravenous cefazolin 1 g every 8 h at day 14 after the initiation of treatment. Despite a detailed medical history from our patient, including his family history, possible contacts such as lizards, reptiles, or fish, and past history of injury, we were unable to identify the source of infection. After the surgical procedure, parameters of inflammatory response as well as pain in the right tibia improved by week 10 after treatments with the appropriate antibiotics. He was discharged after a total of 10 weeks of intravenous antibiotic therapy.

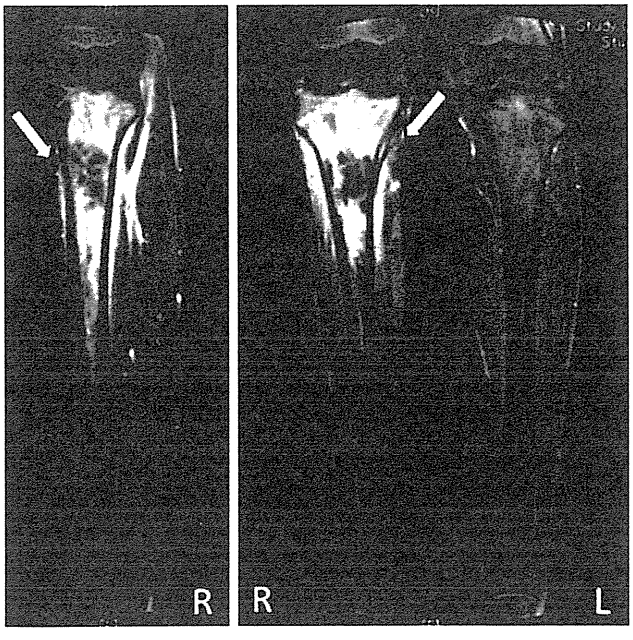

Fig. 1 Fat-suppressed, gadolinium-enhanced T1-weighted magnetic resonance imaging of the lower leg on admission. Heterogeneous high-intensity area was observed in the right tibia and the surrounding soft tissue

Discussion

Of 185,608 isolates identified at our center over the last 7 years, *E. tarda* has only been isolated from five clinical specimens, including four isolates from stool cultures and an isolate from a vaginal discharge, despite the fact that *E. tarda* is an ubiquitous organism with a broad host range. This suggests that the incidence of severe *E. tarda* infection in humans is very low. As shown in the present report, trimethoprim/sulfamethoxazole-resistant pathogens may be selected in patients with CGD, because of the routine prophylaxis with this drug. Interestingly, the patient's brother with X-CGD, who lived with the patient, did not show any clinical manifestations of *E. tarda* infection. The brother had not been treated with antibiotic therapy except for chronic administration of trimethoprim/sulfamethoxazole; however, *E. tarda* was not isolated from his stool culture at 4 months after the patient's osteomyelitis, suggesting that the infection did not spread and occurred within the very limited area.

Trimethoprim/sulfamethoxazole therapy is known to be effective for preventing for severe infections in a patient with CGD [8], and is a broad-spectrum antimicrobial with activity against *Staphylococcus* spp. and gram-negative bacteria, including *Serratia marcescens* and *Burkholderia*

spp. In general, *E. tarda* is susceptible to trimethoprim/sulfamethoxazole, and an *E. tarda* isolate previously identified at our center was also sensitive to it (data not shown). Patients with CGD are given trimethoprim/sulfamethoxazole prophylactically, indicating that there have been no cases of severe *E. tarda* infections reported in CGD patients. However, once *E. tarda* has acquired resistance, it could cause severe infections in patients with CGD, even in the absence of additional predisposing factors. Previously, trimethoprim/sulfamethoxazole was known to be a drug to which microorganisms hardly developed resistance. However, the improper use of multiple antibiotics has made them resistant to trimethoprim/sulfamethoxazole and resulted in treatment failure [9]. Others reported that 30% of *Escherichia coli* (*E. coli*) isolates from patients with urinary tract infections were resistant to trimethoprim/sulfamethoxazole [10]. Non-typhi *Salmonella*, including *Salmonella typhimurium* and *Salmonella enteritidis*, have commonly become resistant to trimethoprim/sulfamethoxazole in southern Africa [11]. A mechanism of resistance to trimethoprim/sulfamethoxazole has not been clarified yet in *E. tarda*, whereas efflux pumps have been considered as a central role of intrinsic resistance to trimethoprim/sulfamethoxazole in *Burkholderia cepacia* that is commonly observed in patients with CGD [12]. So far, there has been no report but for our case that *E. tarda* with resistance to trimethoprim/sulfamethoxazole caused severe infection in a patient with CGD. Since a recent study reported that the rate of antimicrobial resistance has been increasing substantially [10, 11], it is important to keep in mind the prevalence of trimethoprim/sulfamethoxazole-resistant bacilli to maintain appropriate prophylaxis for CGD patients.

Conflict of interest We have documented that we have nothing to disclose.

References

1. Janda JM, Abbott SL. Infections associated with the genus *Edwardsiella*: the role of *Edwardsiella tarda* in human disease. Clin Infect Dis. 1993;17(4):742–8.
2. Jordan GW, Hadley WK. Human infection with *Edwardsiella tarda*. Ann Intern Med. 1969;70(2):283–8.
3. Sonnenwirth AC, Kallus BA. Meningitis due to *Edwardsiella tarda*. First report of meningitis caused by *E. tarda*. Am J Clin Pathol. 1968;49(1):92–5.
4. Golub V, Kim AC, Krol V. Surgical wound infection, tuboovarian abscess, and sepsis caused by *Edwardsiella tarda*: case reports and literature review. Infection. 2010;38(6):487–9. doi: 10.1007/s15010-010-0057-5.
5. Kobayashi S, Murayama S, Takanashi S, Takahashi K, Miyatsuka S, Fujita T, et al. Clinical features and prognoses of 23 patients with chronic granulomatous disease followed for 21 years by a single hospital in Japan. Eur J Pediatr. 2008;167(12):1389–94.
6. Shigemura T, Agematsu K, Yamazaki T, Eriko K, Yasuda G, Nishimura K, et al. Femoral osteomyelitis due to *Cladophialophora arxii* in a patient with chronic granulomatous disease. Infection. 2009;37(5):469–73.
7. Martire B, Rondelli R, Soresina A, Pignata C, Broccoletti T, Finocchi A, et al. Clinical features, long-term follow-up and outcome of a large cohort of patients with chronic granulomatous disease: an Italian multicenter study. Clin Immunol. 2008; 126(2):155–64.
8. Holland SM. Chronic granulomatous disease. Clin Rev Allergy Immunol. 2010;38(1):3–10.
9. Huovinen P. Resistance to trimethoprim–sulfamethoxazole. Clin Infect Dis. 2001;32(11):1608–14.
10. Moreno E, Prats G, Sabaté M, Pérez T, Johnson JR, Andreu A. Quinolone, fluoroquinolone and trimethoprim/sulfamethoxazole resistance in relation to virulence determinants and phylogenetic background among uropathogenic *Escherichia coli*. J Antimicrob Chemother. 2006;57(2):204–11.
11. Morpeth SC, Ramadhani HO, Crump JA. Invasive non-typhi *Salmonella* disease in Africa. Clin Infect Dis. 2009;49(4):606–11.
12. Guglierame P, Pasca MR, De Rossi E, Buroni S, Arrigo P, Manina G, et al. Efflux pump genes of the resistance-nodulation-division family in *Burkholderia cenocepacia* genome. BMC Microbiol. 2006;6:66.

別添１：

同意取得の際に用いられる説明および同意書

患者さんまたは保護者の方へ

「慢性肉芽腫症に対する遺伝子治療臨床研究」

説明文書及び同意書（本人用及び保護者用）

これから「臨床研究」についてご説明します。この「臨床研究」への参加に同意していただけるかどうかは、あなたとあなたのお子さまの自由な意思によるもので、誰からも強要されるものではありません。あなたとあなたのお子さまの参加に同意できない場合には、遠慮なく申し出てください。また、保護者の方が参加に同意した場合でも、あなたのお子さまが拒否した場合は、臨床研究に参加することはできません。ただ、この「臨床研究」への参加に同意していただけない場合でも、今後の診療や治療になんら不利益が生じることはありませんので、ご安心ください。

この説明文書は、研究に参加される 16 歳以上の方を対象としていますので、保護者の方が読まれる場合は、あなたを「あなたのお子さま」と読み替えてください。

目次

1．はじめに …… 297
2．この臨床研究で行う遺伝子治療について …… 298
3．目的 …… 298
4．この研究に参加できる方とできない方 …… 298
5．この臨床研究の方法 …… 299
6．この研究の参加により期待される効果と、予想される不利益 …… 302
7．この臨床研究に参加されない場合の治療法 …… 306
8．臨床研究参加に伴う費用について …… 307
9．健康被害に対する治療と補償について …… 307
10．新たな情報の提供について …… 307
11．プライバシーの保護について …… 307
12．知的財産権の帰属について …… 308
13．保存サンプルに関して …… 308
14．データの二次利用について …… 308
15．お願いしたいこと …… 308
16．臨床研究参加に対する拒否および撤回について …… 309
17．相談窓口 …… 309
《スケジュール》 …… 310
《付録　用語集》 …… 311
同意書 …… 313

1．はじめに

あなたは、医師から今の病状が現在行っている治療だけでは良くならず、また、慢性肉芽腫症に対して有効と考えられるHLA一致造血幹細胞移植もドナー不在などの理由により実施することが難しいとお聞きしていると思います。同時に、医師から新しい治療法としての遺伝子治療について、簡単な説明を受けていると思います。

遺伝子治療は、研究段階の治療法のため、その有効性、安全性について調べています。

そこで、国立成育医療研究センターの免疫科で慢性肉芽腫症の方を対象とした遺伝子治療の臨床研究を行うこととしました。これから、この説明文書を用いて、その内容をご説明します。心配なこと、わからないことがありましたら、遠慮なく、この遺伝子治療を担当する医師にお尋ねください。

なお、この説明文書は、「慢性肉芽腫症に対する遺伝子治療臨床研究」（以下、「臨床研究」とします。）の説明資料であり、慢性肉芽腫症の病気の特徴や一般的な治療方法ならびに遺伝子治療に関しては、**別冊「慢性肉芽腫症についてのパンフレット」**をご覧ください。

この説明文書と同意書の控えは、大切に保管してください。

《臨床研究とは》

現在、日常的に行われている診療では、いろいろな予防法、診断法、治療法の中から安全性や有効性などの点で最善と認められた方法が選択されます。このように標準的な医療が生み出されるためには、前もってその安全性や有効性を、ヒト（患者さんや健康な方）を対象とした科学的検証によって確認する必要があります。そこで、患者さんの生活の質の向上を目的として、医療の標準化を目指した医学研究を「臨床研究」とよびます。

今回の臨床研究は、当センター内に設置された「遺伝子治療臨床研究審査委員会」（倫理委員会）及び国の遺伝子治療審査委員会において、この臨床研究に参加される患者さんの人権保護や安全性確保ならびに科学的に問題がないか等について審査され、上記の点に関して「特段、問題はなく、実施して良い」と承認を受けております。

（独）国立成育医療研究センター遺伝子治療臨床研究審査委員会：平成23年2月24日承認
厚生労働大臣（国の遺伝子治療審査委員会）：平成X年Y月Z日　承認

なお、あなたは、当センター内に設置された「**遺伝子治療臨床研究適応判定委員会**（以下：「適応判定委員会」）」において、臨床研究へ参加することが適切であるか審査されます。また、臨床研究に参加している間、今回の遺伝子治療の安全性、有効性に関して「**遺伝子治療臨床研究評価判定委員会**」において評価されます。